Original Article

OPEN

INFOGRAPHIC

Neutrophil extracellular traps accelerate vascular smooth muscle cell proliferation via Akt/CDKN1b/TK1 accompanying with the occurrence of hypertension

Xinhui Fang[a], Ling Ma[b,c], Yanfu Wang[c], Fang Ren[d], Yanqiu Yu[b], Zhengwei Yuan[c], Hongquan Wei[e], Haipeng Zhang[b], and Yingxian Sun[a]

Objective: Neutrophil extracellular traps (NETs) can trigger pathological changes in vascular cells or vessel wall components, which are vascular pathological changes of hypertension. Therefore, we hypothesized that NETs would be associated with the occurrence of hypertension.

Methods: To evaluate the relationship between NETs and hypertension, we evaluated both the NETs formation in spontaneously hypertensive rats (SHRs) and the blood pressure of mice injected phorbol-12-myristate-13-acetate (PMA) via the tail vein to induce NETs formation in arterial wall. Meanwhile, proliferation and cell cycle of vascular smooth muscle cells (VSMCs), which were co-cultured with NETs were assessed. In addition, the role of exosomes from VSMCs co-cultured with NETs on proliferation signaling delivery was assessed.

Results: Formation of NETs increased in the arteries of SHR. PMA resulted in up-regulation expression of citrullinated Histone H3 (cit Histone H3, a NETs marker) in the arteries of mice accompanied with increasing of blood pressure. NET treatment significantly increased VSMCs count and accelerated G1/S transition *in vitro*. Cyclin-dependent kinase inhibitor 1b (CDKN1b) was down-regulated and Thymidine kinase 1 (TK1) was up-regulated in VSMCs. Exosomes from VSMCs co-cultured with NETs significantly accelerated the proliferation of VSMCs. TK1 was up-regulated in the exosomes from VSMCs co-cultured with NETs and in both the arterial wall and serum of mice with PMA.

Conclusion: NETs promote VSMCs proliferation via Akt/CDKN1b/TK1 and is related to hypertension development. Exosomes from VSMCs co-cultured with NETs participate in transferring the proliferation signal. These results support the role of NETs in the development of hypertension.

Graphical abstract: http://links.lww.com/HJH/C6.

Keywords: exosome, hypertension, neutrophil extracellular traps, thymidine kinase 1, vascular smooth muscle cells

Abbreviations: CDK, cyclin-dependent kinases; CDKN1b, cyclin-dependent kinase inhibitor 1b; cit Histone H3, citrullinated histone H3; DAVID, the Database for Annotation Visualization and Integrated Discovery; DEGs, differentially expressed genes; DMEM, Dulbecco's modified Eagle's medium; FBS, fetal bovine serum; HCD, higher energy collisional dissociation; MBP, mean blood pressure; MPO, myeloperoxidase; NETs, neutrophil extracellular traps; PAD4, peptidyl arginine deiminase 4; PMA, phorbol-12-myristate-13-acetate; PPI, protein–protein interaction; SHR, spontaneously hypertensive rat; TEM, transmission electron microscopy; TK1, thymidine kinase 1; VSMCs, vascular smooth muscle cells; WKY, Wistar–Kyoto rat

INTRODUCTION

Essential hypertension is a major public health issue [1,2]. The cause is complex, involving interactions among genetic and environmental factors [3]. The pathogenesis of essential hypertension is not fully understood [3,4].

Inflammation is closely related to the occurrence and development of hypertension [5–7]. However, the mechanism underlying inflammation-induced hypertension is unclear. Chronic inflammation occurs in a state of low-grade inflammation after an acute inflammatory process when the initiating stimulus is not removed or if the resolution program is disturbed [8]. Chronic inflammation can last for a long time, causing tissue damage, fibrosis, and irreversible organ dysfunction [9,10]. Neutrophils have been shown to play a

Journal of Hypertension 2022, 40:2045–2057

[a]Department of Cardiovascular Medicine, The First Hospital of China Medical University, [b]Department of Pathophysiology, College of Basic Medical Science, [c]Key laboratory of Health Ministry for Congenital Malformation, Department of Pediatric Surgery, [d]Department of Obstetrics and Gynecology, Shengjing Hospital and [e]Department of Otolaryngology, The First Hospital of China Medical University, China Medical University, Shenyang, Liaoning, China

Correspondence to Dr YingXian Sun, Department of Cardiovascular Medicine, The First Hospital of China Medical University, China Medical University, Shenyang, Liaoning 110001, China; E-mail: yxsun@cmu.edu.cn

Received 11 November 2021 **Revised** 10 May 2022 **Accepted** 25 May 2022

DOI:10.1097/HJH.0000000000003231

significant role both in acute and chronic inflammation. Neutrophils are the first line of defense against inflammation. They are recruited to inflammatory sites to eliminate harmful substances. In response to chronic and low-grade inflammatory reactions, neutrophils can form neutrophil extracellular traps (NETs) that cause a particular form of cell death, NETosis, and continue to capture and kill microorganisms, preventing the spread of infection. NETs are formed by the chromatin reticulum, in which a variety of proteins are embedded, such as citrullinated histone H3 (cit Histone H3) and myeloperoxidase (MPO) [11–15].

NETs have been detected in human vascular tissues and are related to vascular wall lesions, such as atherosclerosis [16–20]. Furthermore, NETs can participate in the development of pulmonary hypertension by promoting angiogenesis [20]. Proteins involved in NETs formation, such as peptidyl arginine deiminase 4 (PAD4), can cause fibrosis [21]. Fibrosis is a pathological change in vascular remodeling related to the occurrence and development of hypertension [22]. Moreover, NETs could promote gastric cancer cell proliferation, invasion, migration and epithelial–mesenchymal transition dependent on TGF-β signaling [23]. Furthermore, it has been proved that TNF-α up-regulated neutrophil elastase in vascular smooth muscle cells (VSMCs), which promoted VSMC migration, proliferation and inflammation [24] and mediates the formation of NETs [25]. VSMC proliferation is one of the key vascular pathological changes occurring during the development of hypertension [26].

On the basis of these studies, we hypothesize that NET formation in arteries probably would be related with the development of hypertension by promoting VSMC proliferation. Therefore, the aim of the study is to evaluate the association between arterial NET formation and increasing blood pressure and explore the role of NETs on the cellular and molecular mechanisms of hypertension.

METHODS

Details on the protocol used in this study are shown in the flowchart in Fig. 1.

Animals

Spontaneously hypertensive rat (SHR) and Wistar–Kyoto (WKY) (male, 6 weeks old) were raised to 20 weeks of age to assess the formation of NETs in the arteries under high blood pressure *in vivo*.

In addition, NETs formation in the arteries of BALB/c mice (male, 10–12 weeks old) was induced by phorbol-12-myristate-13-acetate (PMA; Sigma, St Louis, Missouri, USA) [20,27]. PMA (200 μl of 100 nmol/l) were injected in the tail vein once every 3 days for 3 months to induce NET formation.

All animals were obtained from the Animal Center of China Medical University and kept under controlled conditions (light : dark cycle of 12 : 12, starting at 0800 h; 22–23 °C; 45–50% relative humidity).

Blood pressure evaluation

SBP was evaluated in mice at month 0 (basal) and month 3 after PMA injection, and in rats at week 6 and week 20 using a standard tail cuff [28,29].

Immunohistochemistry assay

Sections of superior mesenteric artery of SHR and WKY were blocked with 0.3% hydrogen peroxide, followed by incubation with 5% normal goat serum and then with a rabbit polyclonal anticit Histone H3 antibody at 4 °C overnight. Next, the sections were incubated with the biotinylated secondary antibody. Visualization was performed via the diaminobenzidine reaction and hematoxylin staining. The staining intensities were determined by measurement of the integrated optical density by light microscopy using a computer-based Image-Pro Morphometric System by two independent observers in a double-blind manner.

Neutrophil isolation and neutrophil extracellular trap induction

Neutrophils were isolated from whole blood of Wistar rat and induced by PMA to form NETs *in vitro*. Male 10-week-old Wistar rat was sacrificed and 4 ml whole blood per rat was collected from the left ventricle in EDTA-treated collection tubes. Mature neutrophils were purified by centrifugation for 30 min at 1500*g* on a discontinuous Percoll gradient consisting of 52% (v/v), 69% (v/v), and 78% (v/v) Percoll in PBS. Mature neutrophils were recovered from the interphase between 69 and 78% Percoll and were pelleted. Remaining erythrocytes were lysed using red blood cell lysis buffer. Neutrophils were washed in PBS and pelleted again by centrifugation for 10 min at 300*g* to remove the remaining lysis buffer. NETs formation was induced from neutrophils by overnight stimulation with 100 nmol/l PMA.

Cell culture and treatments

Rat VSMCs were cultured in low glucose Dulbecco's modified Eagle's medium (DMEM) (Gibco, Waltham, Massachusetts, USA) with 10% fetal bovine serum (FBS) (Gibco). VSMCs were cultured with NETs for 24 h (per 1×10^6 VSMCs: NETs induced from 1×10^6 neutrophils). Meanwhile, in another group that VSMCs were cultured with Ang II (10^{-7} mol/l; Sigma), and this group was performed as a positive control.

Cell proliferation

VSMC proliferation was evaluated using the CellTiter 96 One Solution Proliferation Assay (MTS, G3580; Promega, Madison, Wisconsin, USA) in accordance with the manufacturer's guidelines. Cells were seeded in a 96-well tissue culture plate (5×10^3 cells/well). OD values were read at 490 nm.

Cell cycle analysis

Cells were seeded in a six-well tissue culture plate (5×10^5 cells/well). For G0/G1 synchronization, cells were synchronized by serum deprivation for 12 h. After treatment, the cells were collected and washed. Cells were resuspended in a mixture of RNaseA solution (50 μl) and propidium iodide (PI; 450 μl) and incubated for 30 min in the dark. The DNA content was detected by flow cytometry. The percentages of cells in the G0/G1 phase, S phase, and G2/M phase were analyzed.

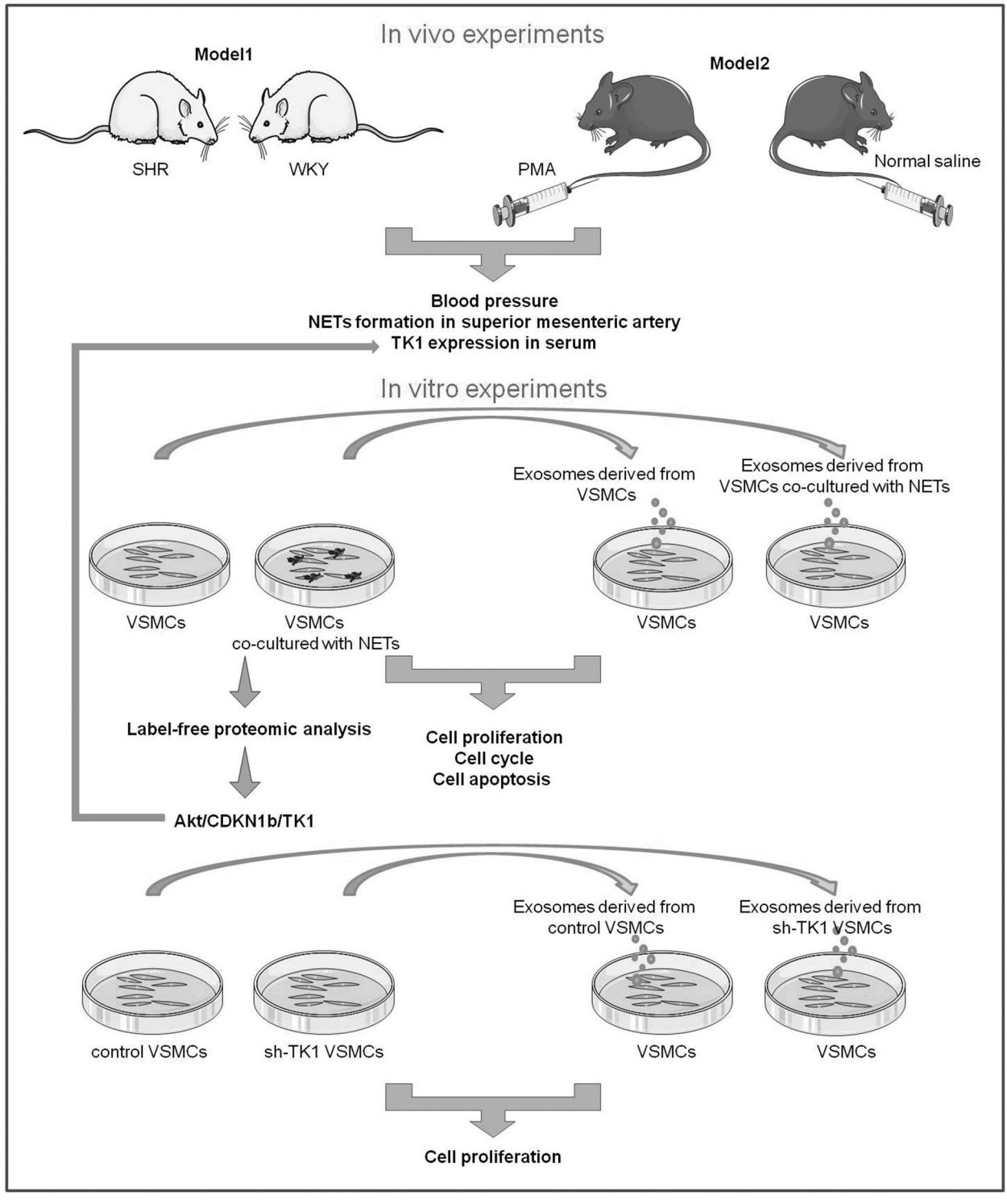

FIGURE 1 Flowchart of the study.

Cell apoptosis assays

Cells were seeded in a six-well tissue culture plate (5×10^5 cells/well). After treatment, cells were collected and washed. Cells were resuspended in 500 μl of binding buffer premixed with 5 μl of Annexin V-FITC and 5 μl of PI and incubated for 15 min at room temperature in the dark. Cells were analyzed with flow cytometry (BD Biosciences, Baltimore, Maryland, USA) within 1 h.

Label-free proteomic analysis

Proteins were extracted using SDT buffer [4% SDS, 100 mmol/l dithiothreitol (DTT), 150 mmol/l Tris–HCl, pH 8.0] and quantified. Approximately, 200 μg of proteins from each sample was supplemented with 30 μl of SDT buffer. After washing with detergent, DTT and other low-molecular-weight components were removed, and cysteine residues were blocked. The protein suspensions were

digested with 4 μg of trypsin (Promega) in 40 μl of 25 mmol/l NH_4HCO_3 buffer, and the resulting peptides were collected. The peptides in each sample were desalted on C18 Cartridges [Empore SPE Cartridges C18 (standard density), bed I.D. 7 mm, volume 3 ml; Sigma, St Louis, Missouri, USA), concentrated by vacuum centrifugation, and reconstituted in 40 μl of 0.1% (v/v) formic acid. The OD_{280} values for the resulting peptides were determined.

Each fraction was injected into the nano liquidchromatography/tandem mass spectrometry (nanoLC-MS/MS) system. The peptide mixture was loaded onto a reverse phase trap column (Thermo Scientific Acclaim PepMap100, 100 μm × 2 cm, nanoViper C18; Waltham, Massachusetts, USA) connected to the C18-reversed phase analytical column (Thermo Scientific Easy Column, 10 cm long, 75 μm inner diameter, 3 μm resin) in buffer A (0.1% formic acid) and buffer B (84% acetonitrile and 0.1% formic acid) at a flow rate of 300 nl/min. The 120 min LC gradient was 0–55% buffer B for 110 min, 55–100% buffer B for 5 min, and 100% buffer B for 5 min.

MS data were acquired using a data-dependent top 10 method, in which the most abundant precursor ions were dynamically chosen from the survey scan (300–1800 m/z) for higher energy collisional dissociation (HCD) fragmentation. The automatic gain control target was set to 3e6, and the maximum inject time was set to 10 ms. The dynamic exclusion duration was 40 s. Survey scans were acquired at a resolution of 70 000 at m/z 200 and resolution for HCD spectra was set to 17 500 at m/z 200, and the isolation width was 2 m/z. Normalized collision energy was 30 eV and the underfill ratio was defined as 0.15. The instrument was run with peptide recognition mode enabled. The MS data were analyzed using MaxQuant version 1.5.3.17 (Max Planck Institute of Biochemistry, Martinsried, Germany).

Bioinformatic analysis

A heatmap was generated to visualize relative protein expression data. The Database for Annotation, Visualization and Integrated Discovery (DAVID) (version 6.8) was used for a Gene Ontology (GO) analysis. The heatmap and GO annotation results were plotted using R scripts. Protein–protein interaction (PPI) information was retrieved using STRING (version 11.5). The results were downloaded in the XGMML format and imported into Cytoscape5 for visualization and further hub genes analysis.

TK1 gene silencing

TK1 expression was inhibited by using Hu6-MSC-CMV-GFP-SV40-Neomycin vectors and two siRNA sequences targeting *TK1* (target sequence of siRNA sequence 1: GCGGACAAGTACCACTCTGTT and target sequence of siRNA sequence 2: GTGCTTTCGAGAAGCTTCCTA). In parallel, an unrelated siRNA was designed as a negative control. Plasmid transfection was performed using Lipofectamine 3000 (L3000015; Invitrogen, Carlsbad, California, USA).

Exosome isolation and purification

Using sequential ultracentrifugation, exosomes were collected from the culture medium of VSMCs, VSMCs cultured with NETs, and TK1 silencing VSMCs, respectively. Briefly, the cell culture medium was centrifuged at 200*g* for 20 min and 2000*g* for 20 min and the supernatants were filtered by a 0.22 μm filter. The filtrates were collected for centrifugation at 10 000*g* for 1 h and 100 000*g* for 4 h. The final pellet containing exosomes was resuspended in PBS and used for transmission electron microscopy (TEM), western blotting of CD9 and Alix (two exosome markers), and an exosome diameter analysis. Then the exosomes were subsequently added into VSMC culture medium to observe the role of the exosomes.

Transmission electron microscopy

Exosomes were fixed with 2% glutaraldehyde in 0.1 mol/l PBS (pH 7.4). Fixed samples were placed on 100 mesh carbon and formvar-coated nickel grids for about 30 min. After samples were washed with several drops of ultra-pure water, 2% uranyl acetate was pipetted on the grids and incubated for 7 min. Excess solution was removed. The grid was washed twice and dried. Images were obtained by TEM (80 kV, 60 000×, H-7650; HITACHI, Tokyo, Japan).

Laser particle size analyzer

The particle size was assessed using the Laser Particle Size and Zeta Potential Analyzer (Nano ZS90; Malvern Instruments, Malvern, UK). Nanoparticles were diluted (1 : 10) with deionized water prior to analyses.

Western blot analysis

Lysates from exosomes, cells, and arterial tissues were prepared with RIPA lysis buffer. Protein lysate and serum of mice injected PMA, SHR and WKY were resolved by 10% SDS–PAGE and electrotransferred to polyvinylidene difluoride membranes. Membranes were blocked with 5% milk for 2 h at room temperature and incubated with primary antibodies at 4 °C overnight [anti-CD9 (1 : 1000, Abcam, ab92726], anti-Alix (1 : 1000, Abcam, ab275377), anti-TK1 (1 : 500, Proteintech, 15691–1-AP), anti-CDKN1b (1 : 500, Proteintech, 25614–1-AP), anti-TOP2a (1 : 500, Abcam, ab52934), anticitrullinated histone H3 (1 : 1000, Abcam, ab5103), anti-MPO (1 : 1000, Abcam, ab208670) and GAPDH (1 : 5000, Proteintech, 10494–1-AP). After incubation with the horseradish peroxidase-conjugated secondary antibody and washing, blots were developed with chemiluminescent reagents (WBKIS0100; Millipore, Billerica, Massachusetts, USA).

Statistical analysis

Differentially expressed proteins between VSMCs and VSMCs co-cultured with NETs were identified based on a fold change greater than 2 and P less than 0.05 using the Wilcoxon rank sum test. Gene ontology enrichment was determined based on the Fisher's exact test. Benjamini–Hochberg correction was applied for multiple testing. Only functional categories with P values of less than 0.05 were considered significant.

Statistical analyses were performed using SPSS 22.0 (IBM, Armonk, New York, USA). Results are presented as means ± SEM. Differences between two groups were analyzed with Student's t tests. Differences among multiple groups were analyzed with one-way ANOVA. For all statistical comparisons, P less than 0.05 was considered significant.

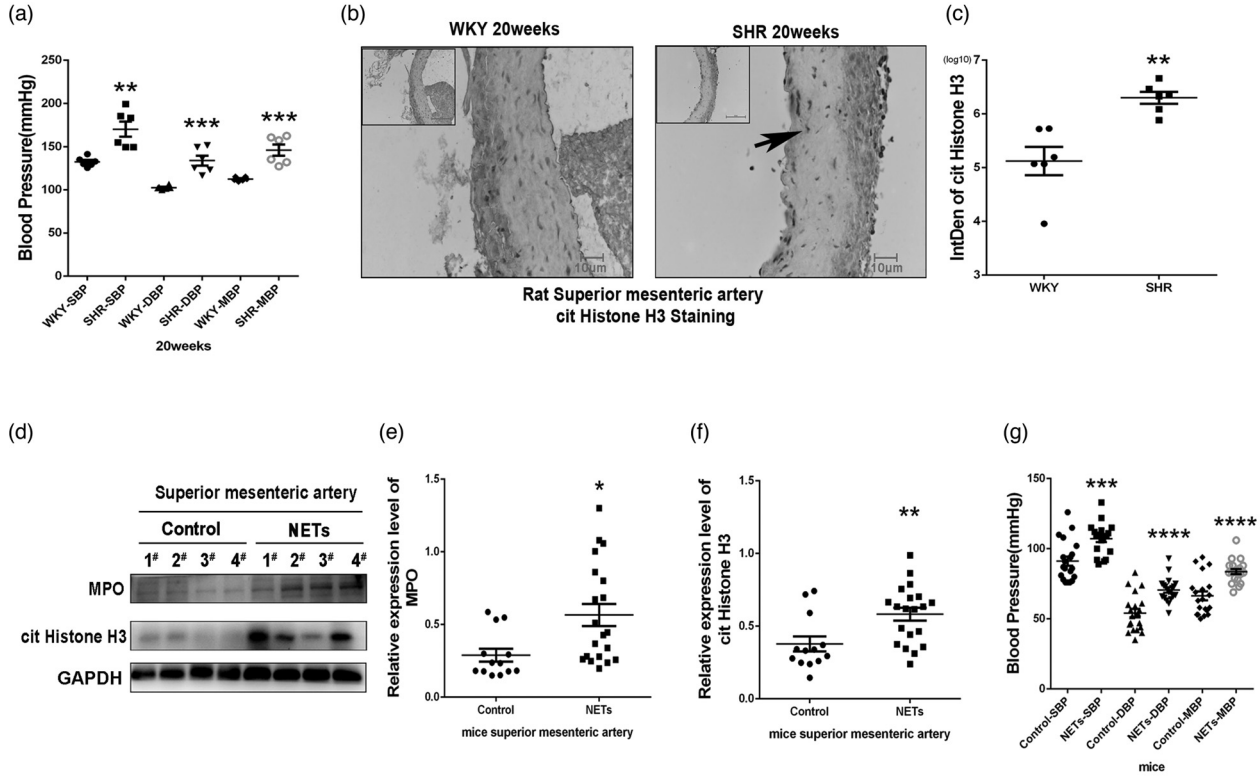

FIGURE 2 The formation of neutrophil extracellular traps in the vascular wall is related to the occurrence of hypertension. (a) The blood pressure of SHR and WKY rats was detected at week 20. (b) Immunohistochemical detection of cit Histone H3 expression in the superior mesenteric artery of WKY and SHR rats. NETs formed in the subintima and between smooth muscle tissues of SHR artery (arrow). (c) The histogram shows statistical analysis of cit Histone H3 expression level in the rat superior mesenteric artery. (d) MPO, cit Histone H3 (both NET markers), and GAPDH (an internal reference) expression in the superior mesenteric artery of mice were tested by western blot analysis. NETs in artery were quantitatively assessed by the expression levels of MPO and cit Histone H3. (e) The histogram shows statistical analysis of MPO expression level in the rat superior mesenteric artery. (f) The histogram shows statistical analysis of cit Histone H3 expression level in the rat superior mesenteric artery. (g) The blood pressure of NETs induced mice and control mice ($^{*}P < 0.05$, $^{**}P < 0.01$, $^{***}P < 0.001$, $^{****}P < 0.0001$). MPO, myeloperoxidase; NETS, neutrophil extracellular traps; SHR, spontaneously hypertensive rat, WKY, Wistar–Kyoto rat.

RESULTS

Neutrophil extracellular trap formation increased in arterial wall with hypertension in spontaneously hypertensive rat model

To explore the close relationship between the formation of NETs in arterial wall and the occurrence of hypertension, we assessed the NETs formation in the arteries of the SHR model. First, blood pressure [including SBP, DBP, and mean blood pressure (MBP)] was measured at 20 weeks in SHR. WKY rats were as control. At 20 weeks, blood pressure was higher in SHR than in WKY rats (SHR vs. WKY: $P_{SBP} = 0.002$, $P_{DBP} = 0.0004$, $P_{MBP} = 0.0005$, $n = 6$) (Fig. 2a) Moreover, cit Histone H3 staining, a marker of NET formation was detected (Fig. 2b). The expression of cit Histone H3 in the superior mesenteric artery was higher in SHR than that in WKY rats (SHR vs. WKY: $P = 0.0022$, $n = 6$) (Fig. 2c). The increase in blood pressure in SHR is caused by genetic factors as we detected an increase formation of NETs in their arteries of SHR.

The formation of neutrophil extracellular traps in the artery was accompanied by hypertension

To explore the role of NETs on blood pressure *in vivo*, NETosis was induced in vessels by injecting of PMA in the tail vein of mice. Mice injected with physiological saline were used as the control. After 3 months of sustained blood vessels low-dose inflammation, western blotting revealed that the NETs markers MPO and cit Histone H3 were upregulated in the superior mesenteric artery of mice with NETs formation (Fig. 2d). The expression level of MPO (NETs group vs. control group: $P = 0.0107$, NETs: $n = 20$, control: $n = 13$), cit Histone H3 (NETs vs. control: $P = 0.0058$, NETs: $n = 20$, control: $n = 13$) in the superior mesenteric artery was elevated in mice injected of PMA (Fig. 2e and f). When blood pressure was measured. The SBP, DBP, and MBP were significantly higher than those in the group receiving physiological saline as control (NETs group vs. control group: $P_{SBP} = 0.0004$; $P_{DBP} < 0.0001$; $P_{MBP} < 0.0001$, NETs: $n = 20$, control: $n = 20$) (Fig. 2g). NET formation in PMA-injected mice was accompanied by an increase in blood pressure, indicating that NET formation is related to increasing blood pressure.

Neutrophil extracellular traps promote vascular smooth muscle cell proliferation and expedite the G1 to S phase transition

To study the effect of NETs on blood pressure, we further explored their effect of NETs on VSMC proliferation, cell cycle progression, and apoptosis. First, neutrophils were

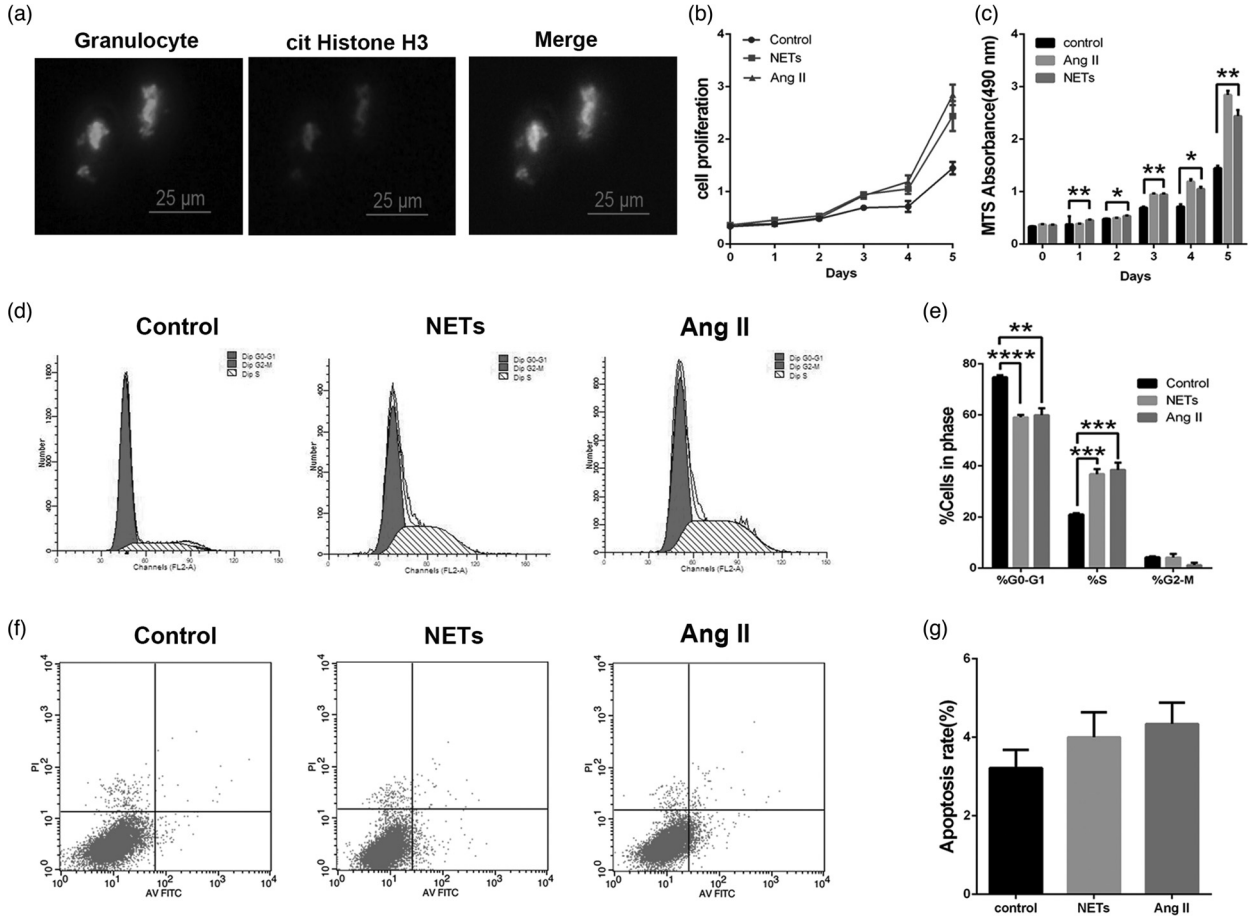

FIGURE 3 Neutrophil extracellular traps promote proliferation and cell cycle progression and do not increase apoptosis in vascular smooth muscle cells in *vitro*. (a) The formation of NETs was identified by immunofluorescence staining Granulocyte and cit Histone. (b) Cell viability over 5 days was determined by the MTS method and cell proliferation curve. (c) The histogram shows statistical analysis of cell growth determined by OD values. (d) Cell cycle analysis of VSMCs (control), VSMCs cultured with NETs (NETs) and VSMCs cultured with Ang II (Ang II) by PI staining, respectively. (e) The histogram shows statistical analysis for cell cycle. (f) Detection of apoptosis of VSMCs (control), VSMCs cultured with NETs (NETs) and VSMCs cultured with Ang II (Ang II) by annexin V and PI double staining, respectively. (g) The histogram shows statistical analysis for cell apoptosis by analyzing apoptosis rate ($^{**}P < 0.01$, $^{***}P < 0.001$, $^{****}P < 0.0001$). NETS, neutrophil extracellular traps; VSMCs, vascular smooth muscle cells.

extracted and then NETs formation was induced *in vitro* using PMA. The formation of NETs was confirmed via immunofluorescence staining of Granulocyte and cit Histone H3 (Fig. 3a). Then, VSMCs were cultured with NETs. NETs significantly increased VSMC proliferation from day 1 to 5 compared with proliferation rate in the control group (NETs group vs. control group: the first day $P = 0.007$, the second day $P = 0.049$, the third day $P = 0.006$, the fourth day $P = 0.039$, the fifth day $P = 0.0089$, $n = 6$) (Fig. 3b). AngII is known to promote VSMC proliferation [18]. As expected, we found that treatment with AngII treatment resulted in a significantly higher rate of proliferation from days 3 to 5 than the rates in the control group (Fig. 3b and c).

The rapid proliferation of VSMCs induced by NETs might be caused by the acceleration of cell cycle progression or inhibition of apoptosis. We found that NETs decreased the proportion of cells in the G1 phase and increased that in the S phase. Similarly, AngII decreased the proportion of VSMCs in G1 and increased that in the S phase (NETs group vs. control group, $P_{\text{G1 phase}} = 0.0066$ and $P_{\text{S phase}} = 0.0049$, $n = 4$) (Fig. 3d and e). Compared with the control, there were no differences in the rate of apoptosis relative to controls between NETs-treated and AngII-treated VSMCs at various apoptosis stages ($n = 4$) (Fig. 3f and g). These findings suggest that NETs facilitate VSMC proliferation, and this effect is mediated, at least in part, by the promotion of the G1/S transition and is not related to a reduction in apoptosis.

Proteomic and bioinformatics analyses and Immunological validation

A label-free proteomic analysis was used to identify differentially expressed proteins between VSMCs and VSMCs stimulated with NETs to explore the molecular mechanisms underlying the effect of NETs on VSMC proliferation. A hierarchical clustering analysis showed that 141 proteins were differentially expressed between NET-treated VSMCs and VSMCs, including 25 up-regulated proteins in NET-treated VSMCs, 18 down-regulated proteins in NET-treated VSMCs (Fig. 4a), 44 proteins expressed specifically in NET-treated VSMCs, and 54 proteins expressed specifically in VSMCs (Fig. 4b). Of note, CDKN1b, which inactivates

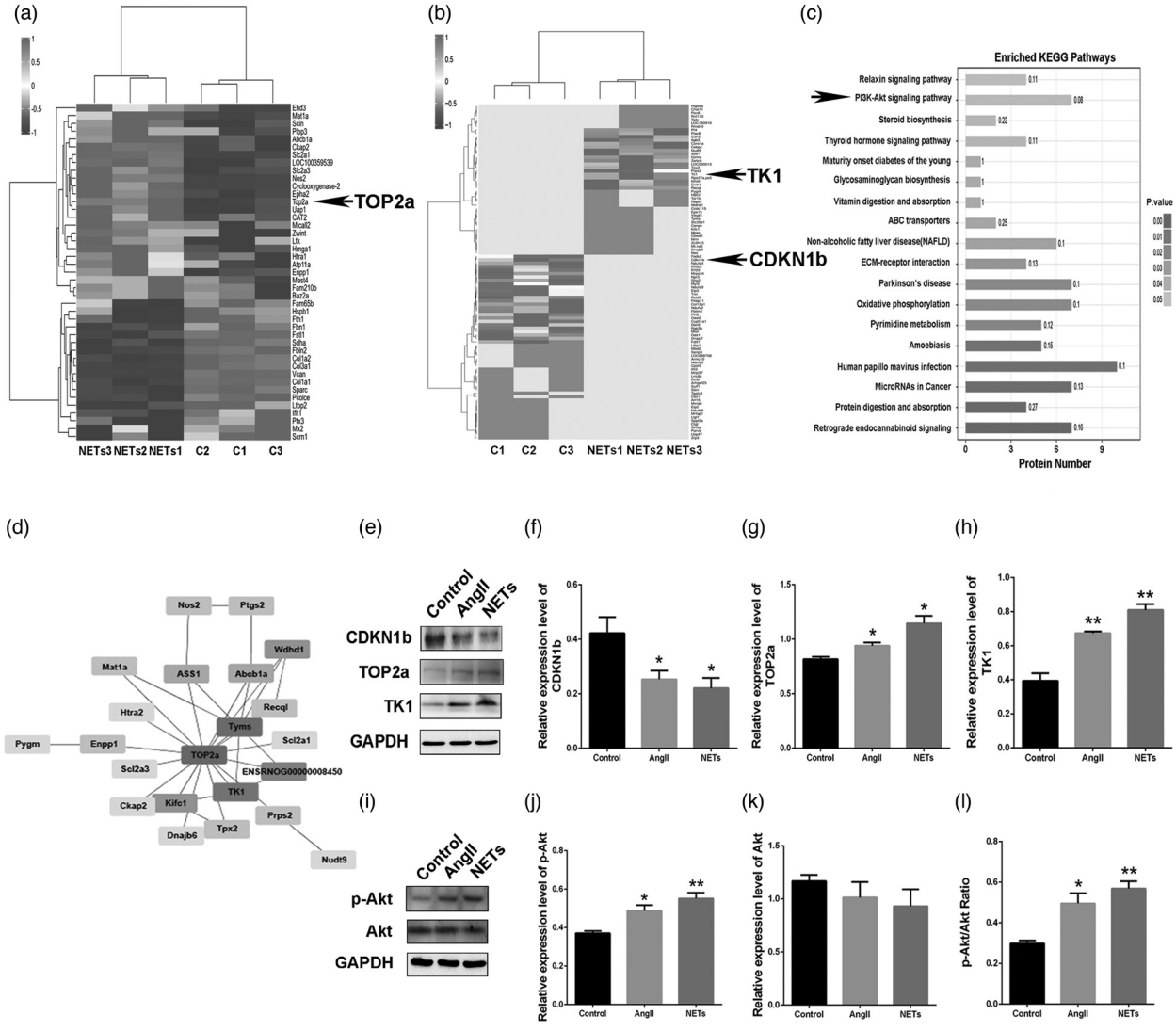

FIGURE 4 Proteomic and bioinformatics analyses of differentially expressed proteins in vascular smooth muscle cells with or without neutrophil extracellular trap treatment. (a) Heatmap and hierarchical clustering revealed differentially expressed proteins between VSMCs with or without NETs treatment. (b) Hierarchical clustering revealed specific differentially expressed proteins in the two groups. (c) Pathway analyses of common and specific differentially expressed proteins. (d) Hub gene analyses of up-regulated proteins, including both common and specific differentially expressed proteins. In this analysis, node color represents the number of links between a protein and other proteins within the network (where colors from dark gray to light gray indicate more to fewer links). (e) Protein expression levels of CDKN1b in VSMCs with NETs treatment compared with untreated VSMCs. Additionally, VSMCs treated with Ang II were evaluated as a positive control. GAPDH was selected as a reference protein. Histograms show statistical analysis for the relative expression of CDKN1b (f), TOP2a (g), and TK1 (h). (I) Phosphorylated Akt (p-Akt) and total Akt levels in VSMCs, NET-treated VSMCs, and AngII-treated VSMCs. Histograms show statistical analysis for the relative expression of p-Akt (j), the relative expression of Akt (k), and p-Akt/Akt Ratio (l) (*$P < 0.05$, **$P < 0.01$). NETs, neutrophil extracellular traps; TK1, thymidine kinase 1; VSMCs, vascular smooth muscle cells.

cyclin-dependent kinases (CDK) when bound and induces cell cycle arrest at the G1/S check point, was only detected in the control group and not in VSMCs cultured with NETs. Furthermore, a pathway enrichment analysis showed that the PI3K-Akt pathway was enriched in VSMCs after NET stimulation. The activation of the PI3K-Akt pathway is known to promote cell growth via the inhibition of CDKN1b (Fig. 4c) [30]. To identify candidate differentially expressed proteins with critical roles in VSMCs after NETs stimulation, all significantly upregulated differentially expressed proteins were used for a PPI network analysis, and 13 hub genes were identified and used to construct a co-expression network (Fig. 4d). In the co-expression network, TOP2a was a central component. TK1, expressed specifically in VSMCs cultured with NETs, was a neighboring protein that directly interacted with and was controlled by TOP2a. TK1 is related to cell proliferation. It catalyzes the addition of a gamma-phosphate group to thymidine to create dTMP, which is the first step in the biosynthesis of dTTP, required for DNA replication. On the basis of our bioinformatic analysis, the PI3K/Akt/CDKN1b-signaling axis was activated by NETs in VSMCs based on our bioinformatic analysis. TOP2a expression increased and positively regulated *TK1* after the inhibition of CDKN1b.

To validate the results of the proteome analysis, CDKN1b, TOP2a, and TK1 were analyzed using western blotting. Levels of CDKN1b were lower and levels of TOP2a and TK1 were higher in the NETs-treated group than in the control group, CDKN1b (NETs group vs. control group: $P = 0.0276$, $n = 4$), TOP2a (NETs group vs. control group:

$P = 0.0105$, $n = 3$), and TK1 (NETs group vs. control group: $P = 0.0018$, $n = 3$) (Fig. 4e–h). For the three proteins, similar trends were observed in the label-free proteomic analysis and in the western blots. The effects of AngII on levels of the three proteins were similar to the effects of NETs. The PI3K/Akt/CDKN1b-signaling axis contributed to the proliferation induced by NETs. Levels of phosphorylated Akt and phosphorylated Akt/Akt were significantly increased (NETs group vs. control group: phosphorylated Akt, $P = 0.0049$, $n = 3$) (NETs group vs. control group: phosphorylated Akt/Akt, $P = 0.0022$, $n = 3$), whereas the expression of total Akt was unchanged (Fig. 4i–l). AngII and NETs had similar effects on VSMCs.

Neutrophil extracellular traps promote vascular smooth muscle cells proliferation via TK1

RNAi was used to knockdown TK1 in VSMCs. Two TK1-specific RNAi fragments (shTK1–1 and shTK1–2) were transfected into VSMCs and the downregulation of TK1 was confirmed by western blotting (shTK1–1 vs. NC: $P = 0.0173$, $n = 3$, shTK1–2 vs. NC: $P = 0.0398$, $n = 3$) (Fig. 5a and b). After TK1 was knocked down, cell proliferation decreased (the fourth day: shTK1–1 vs. NC: $P = 00161$, $n = 4$; the fifth day: shTK1–1 vs. NC: $P = 0.008$, $n = 4$, shTK1–1 vs. NC: $P = 0.0089$, $n = 4$) (Fig. 5c and d). Furthermore, the NET-induced increase in VSMC proliferation was blocked by TK1 knockdown in VSMCs (the first day: shTK1–1+NETs vs. NC+NETs, $P < 0.0001$, shTK1–2+NETs vs. NC+NETs $P = 0.0005$; the second day: shTK1–1+NETs vs. NC+NETs $P = 0.0102$; the third day: shTK1–1+NETs vs. NC+NETs, $P = 0.0469$, shTK1–2+NETs vs. NC+NETs $P = 0.0408$; the fourth day: shTK1–1+NETs vs. NC+NETs $P = 0.0166$; the fifth day: shTK1–1+NETs vs. NC+NETs, $P = 0.0002$, shTK1–2+NETs vs. NC+NETs, $P < 0.0001$, $n = 4$) (Fig. 5a and f).

Exosomes derived from vascular smooth muscle cells proliferation-neutrophil extracellular traps cultured promote vascular smooth muscle cell proliferation and cell cycle progression by transferring TK1

We hypothesized that exosomes might transmit proliferation signals from VSMCs in contact with NETs to those not in contact [31–33]. To evaluate this hypothesis, exosomes derived from the VSMC culture medium were isolated by ultracentrifugation and identified by TEM, a laser particle size analyzer, and western blotting. TEM revealed that exosomes had a cup-shaped morphology (Fig. S1A, http://links.lww.com/HJH/C3). As determined using a laser particle size analyzer, most particles were approximately 50–150 nm in diameter with a peak at around 100 nm (Fig. S1B, http://links.lww.com/HJH/C3). The exosomal protein markers Alix and CD9 were detected in these fractions (Fig. S1C, http://links.lww.com/HJH/C3).

Cell proliferation, cell cycle progression, and apoptosis in VSMCs treated with exosomes derived from VSMCs (exosome group) and VSMCs treated with exosomes derived from NETs-treated VSMCs (NETs exosome group) were evaluated. VSMCs cultured with NETs exosomes showed significantly greater proliferation than that in the exosome group (NETs exosome group vs. exosome group: the third day $P = 0.0016$, the fifth day $P = 0.0101$, $n = 4$; exosome group vs. control group: the fourth day $P = 0.0008$, the fifth day $P = 0.006$, $n = 4$) (Fig. 6a and b). The exosome group showed increased proliferation compared with the control group.

Furthermore, a cell cycle analysis using flow cytometry revealed that the exosome group had a lower proportion of cells in the G1 phase and higher proportion of cells in the S phase than those in the control group (exosome group vs. control group: $P_{\text{G1 phase}} = 0.0291$, $P_{\text{S phase}} = 0.0133$, $n = 4$; NETs exosome group vs. exosome group: $P_{\text{G1 phase}} = 0.001$, $P_{\text{S phase}} < 0.0001$, $n = 4$) (Fig. 6c and d). The proportion of cells in G1 was lower and the proportion of cells in the S phase was higher in the NETs exosome group than those in the exosome group. These findings indicated that NETs promoted the G1/S transition (Fig. 6c and d).

There were no differences in the rate of apoptosis at various stages among the three groups ($n = 4$) (Figs. S2A and S2B, http://links.lww.com/HJH/C4). These findings suggest that exosomes from VSMCs facilitated VSMC proliferation and promoted the G1/S transition, without affecting apoptosis. Moreover, exosomes derived from NET-treated VSMCs had greater effects than those from VSMCs.

After NET stimulation, TK1 was up-regulated in VSMC-derived exosomes (exosomes derived from NETs treated VSMCs vs. exosomes derived from VSMCs: $P = 0.0086$, $n = 4$) (Fig. 6e and f). We hypothesized that the exosome-induced increases in VSMC proliferation were mediated by TK1 signaling. To explore this, exosomes from VSMCs in which TK1 was knocked down were isolated. With the knockdown of TK1 in VSMCs, exosomal TK1 was concurrently downregulated (shTK1–1 vs. NC: $P = 0.0083$, $n = 3$; shTK1–2 vs. NC: $P = 0.0125$, $n = 3$) (Fig. 6g and h). In VSMCs cultured with these exosomes, the rate of proliferation was significantly lower than that of VSMCs cultured with VSMC-derived exosomes without TK1 knockdown (the fourth day: VSMCs + shTK1–2 vs. VSMCs + NC exosomes, $P = 0.0232$; the fifth day: VSMCs + shTK1–1 vs. VSMCs + NC exosomes, $P = 0.0044$, VSMCs + shTK1–2 vs. VSMCs + NC exosomes, $P = 0.0002$, $n = 4$) (Fig. 6i and j).

TK1 was up-regulated in the artery and serum of mice with phorbol-12-myristate-13-acetate-induced neutrophil extracellular traps formation

Our results showed that NETs promote cell proliferation by up-regulating the expression of TK1 in VSMCs *in vitro*. We then evaluated whether NETs induce the upregulation of TK1 in the arteries, indicating a NETs-induced increase in VSMC proliferation. TK1 expression was evaluated in the arteries of mice injected with PMA to induce arterial NET formation. TK1 protein levels were found to be increased both in PMA-treated mouse arteries (NETs vs. control: $P_{\text{TK1}} = 0.0403$) (Fig. 7a and b) and serum (NETs vs. control: $P_{\text{TK1}} = 0.0015$) (Fig. 7c and d). Meanwhile, the TK1 expression in serum of SHR and WKY were assessed. And the result showed that there are no difference between SHR and WKY (Fig. S3a and b, http://links.lww.com/HJH/C5).

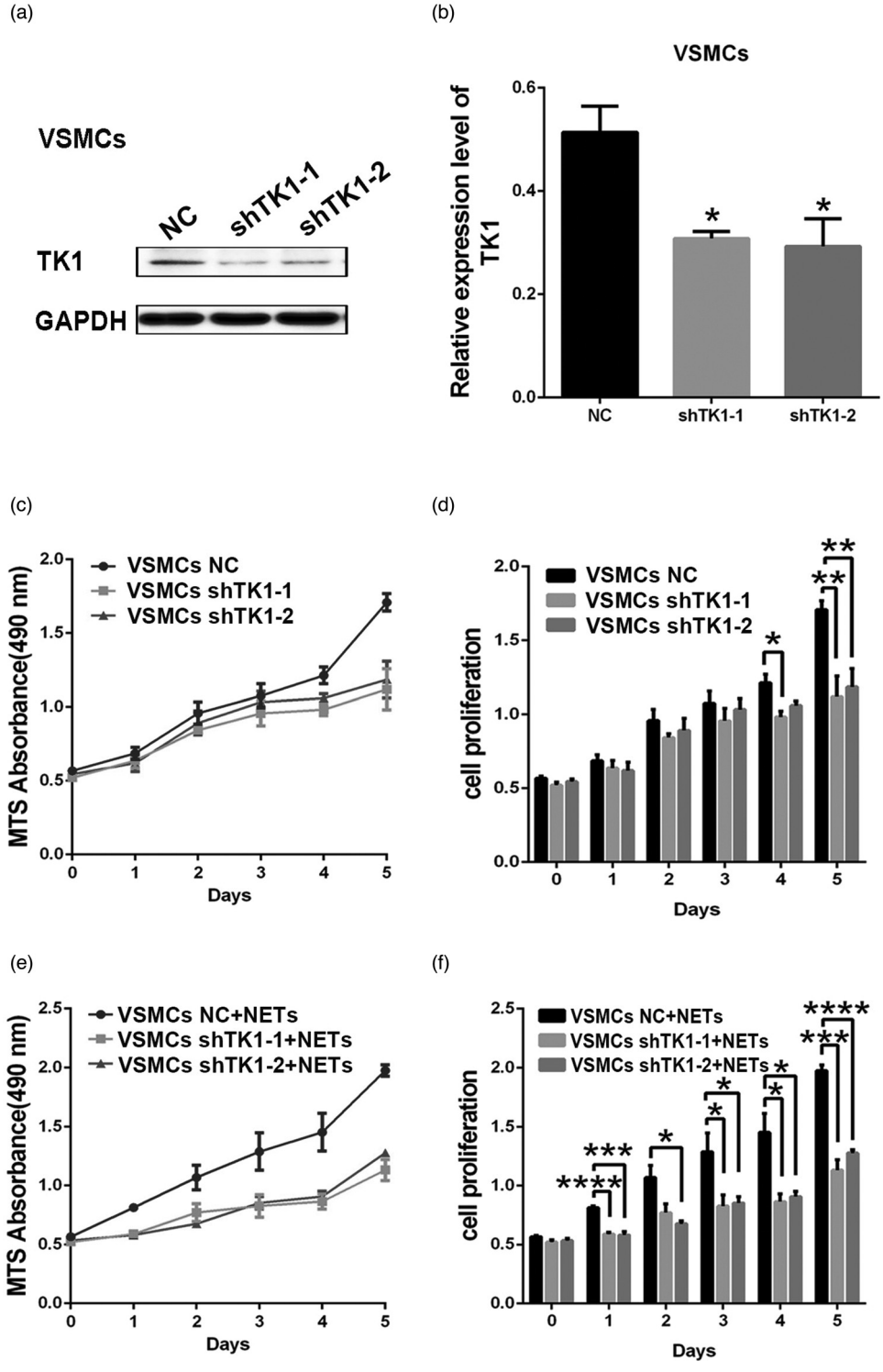

FIGURE 5 Neutrophil extracellular traps accelerate vascular smooth muscle cell proliferation via thymidine kinase 1. (a) Western blot analysis of TK1 expression in VSMCs after TK1 knockdown by siRNA-TK1. (b) Histogram shows statistical analysis of TK1 expressed after TK1 knockdown in VSMCs. (c) Proliferation of VSMCs after TK1 knockdown was assessed by MTS assays. (d) Histogram shows statistical analysis of cell growth of VSMCs after TK1 knockdown by OD values. (e) Proliferation of TK1 knockdown VSMCs with NET treatment. (f) The histogram shows statistical analysis of cell growth TK1 knockdown VSMCs with NETs treatment by OD values. (*$P < 0.05$, **$P < 0.01$, ***$P < 0.001$, ****$P < 0.0001$). NETs, neutrophil extracellular traps; TK1, thymidine kinase 1; VSMCs, vascular smooth muscle cells.

DISCUSSION

In this study, we hypothesized that NET formation in artery probably may be related to the development of hypertension. On the basis of this hypothesis, NET formation was tested in the SHR model. Our data show that there was NET formation in the arteries of hypertensive rats. Moreover, in the mouse model, PMA was used to induce

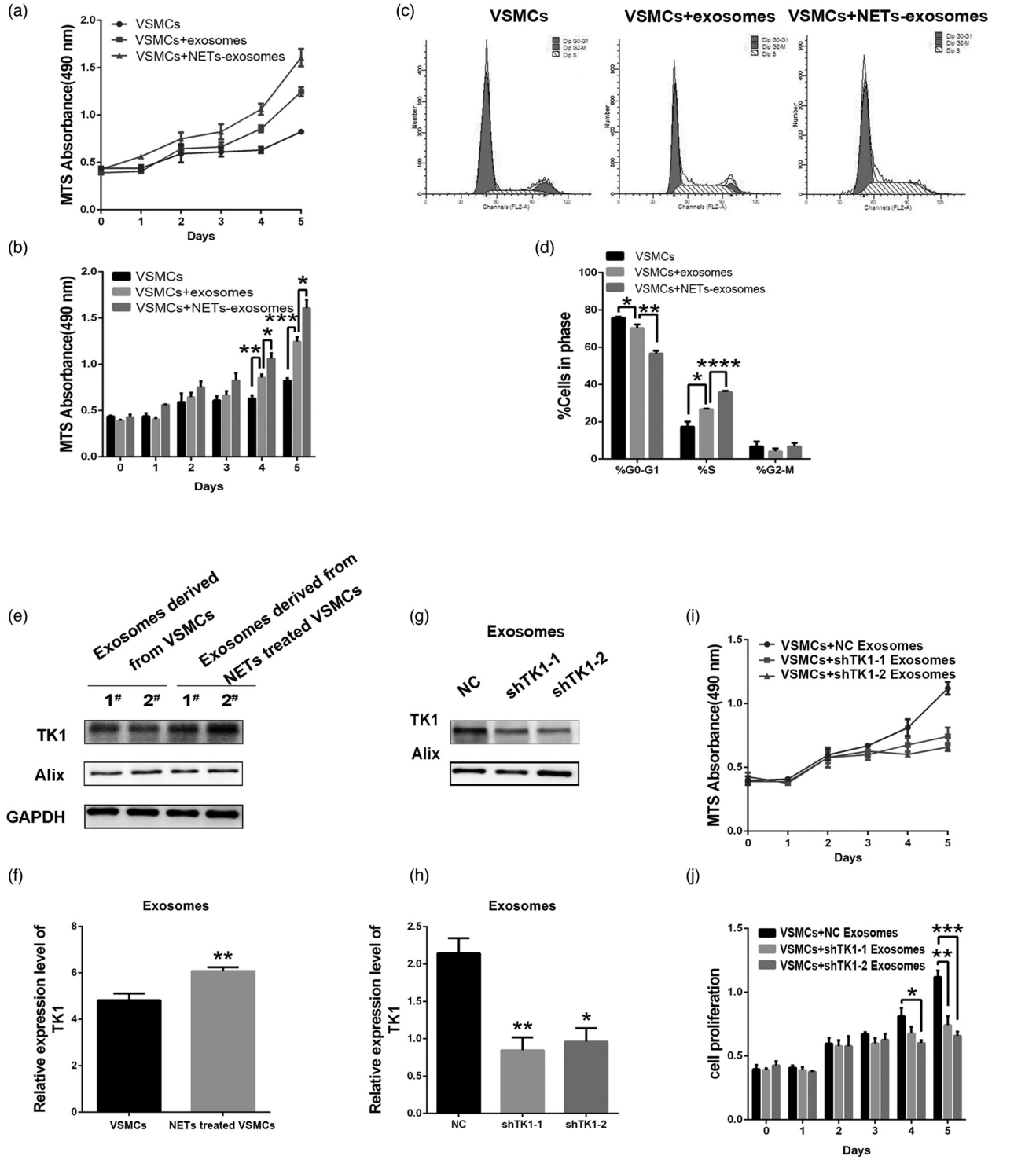

FIGURE 6 Exosomes derived from vascular smooth muscle cells with neutrophil extracellular trap treatment accelerate vascular smooth muscle cell proliferation via TK1 and promote vascular smooth muscle cell cycle progression. (a) Proliferation of VSMCs, VSMCs treated with exosomes derived from VSMCs and VSMCs treated with exosomes derived from VSMCs with NETs treatment were assessed by MTS assays, respectively. (b) The histogram shows statistical analysis of cell growth of VSMCs and VSMCs treated with exosomes derived from VSMCs with NETs treatment by OD values. (c) Cell cycle analysis of VSMCs, VSMCs treated with exosomes derived from VSMCs and VSMCs treated with exosomes derived from VSMCs with NETs treatment by PI staining. (d) The histogram shows statistical analysis of cell cycle of VSMCs, VSMCs treated with exosomes derived from VSMCs and VSMCs treated with exosomes derived from VSMCs with NETs treatment. (e) TK1 expression was analyzed in exosomes derived from VSMCs with NET treatment and exosomes derived from VSMCs by western blot analysis. Alix, an exosomal marker, was detected as a reference protein, and GAPDH was included as a control. (f) The histogram shows statistical analysis of TK1 expressed in exosomes derived from VSMCs with NETs treatment and exosomes derived from VSMCs. (g) After TK1 knockdown in VSMCs, western blotting was performed to detect exosomal TK1 expression. (h) The histogram shows statistical analysis of TK1 expression in exosomes derived from VSMCs after TK1 konckdown. (i) Proliferation of VSMCs treated with exosomes derived from VSMCs and VSMCs treated with exosomes derived from VSMCs with TK1 knockdown were assessed by MTS assays, respectively. (j) The histogram shows statistical analysis of cell growth of VSMCs treated with exosomes derived from VSMCs and VSMCs treated with exosomes derived from VSMCs with TK1 knockdown by OD values ($^{*}P < 0.05$, $^{**}P < 0.01$, $^{***}P < 0.001$, $^{****}P < 0.0001$). NETs, neutrophil extracellular traps; TK1, thymidine kinase 1; VSMCs, vascular smooth muscle cells.

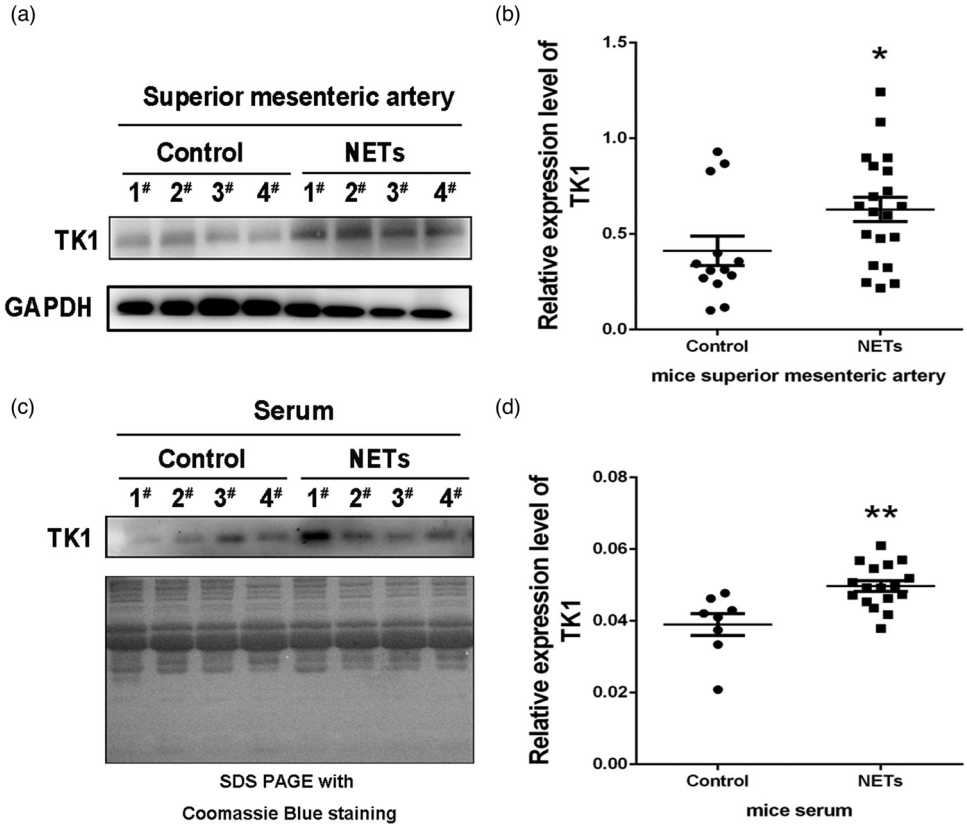

FIGURE 7 Thymidine kinase 1 expression was tested in the artery and serum of mice with neutrophil extracellular trap formation in arteries induced by phorbol-12-myristate-13-acetate. (a) Western blot analysis of TK1 expression in the superior mesenteric artery of mice injected with PMA to induce NETs formation in artery and control mice injected with physiological saline. (b) The histogram shows statistical analysis of TK1 expressed in the superior mesenteric artery of mice with NETs induced and control mice. (c) Western blot analysis of TK1 expression in the serum of mice injected with PMA and control mice injected with physiological saline. (d) The histogram shows statistical analysis of TK1 expressed in serum of mice with NETs induced and control mice ($^{*}P < 0.05$, $^{**}P < 0.01$). NETs, neutrophil extracellular traps; PMA, phorbol-12-myristate-13-acetate; TK1, thymidine kinase 1.

the formation of NETs in the vascular wall, and the blood pressure of mice increased, indicating that NETs was related to the increase of blood pressure. To note, PMA also is a potent oxidative stress inducer, so the role of PMA on blood pressure should be considered.

Our in-vitro experiments demonstrated that NETs promote the G1/S transition and facilitate VSMC proliferation. Meanwhile, in this study, Ang II was used as positive control. That was as Ang II was able to promote the proliferation of vascular endothelial cells [34] and participated in the occurrence of hypertension [35]. And it was confirmed that Ang II was able to trigger the release of NETs, linking thromboinflammation with essential hypertension [36]. A label-free proteomics analysis provided insight into the molecular mechanism by which NETs promote VSMC proliferation. In particular, CDKN1b, a key kinase that suppresses cell cycle progression through the G1/S checkpoint, was downregulated in the NET-treated group and promoted the G1/S transition, consistent with the phenotypic alterations. The PI3K-Akt pathway was identified as a key pathway contributing to NET-induced alterations based on a gene ontology analysis. Previous studies have confirmed that cell proliferation can be positively regulated by the activation of the PI3K/Akt/CDKN1b-signaling axis [30]. Our findings suggest that NETs promote VSMC proliferation by accelerating the G1/S transition via the PI3K/Akt/CDKN1b-signaling axis. TK1 is a diagnostic biomarker for many types of cancer [37–40]. After the downregulation of CDKN1b, E2F promotes *TK1* transcription. Our results show that TK1 was upregulated in proliferating VSMCs treated with NETs and the rapid proliferation of VSMCs was blocked by TK1 knockdown. Therefore, we conclude that TK1 promotes the proliferation stimulated by NETs via the PI3K/Akt/CDKN1b-signaling axis.

Exosomes are heterogeneous molecules with diameters of 30–200 nm. Exosomes reflect the phenotypic state of the parent cells from which they are generated. Exosomes can transfer proteins between cells and affect the biological behaviour of recipient cells through modulating signaling pathways in recipient cells [41]. Our finding demonstrated that the rapid proliferation of VSMCs induced by NETs can be transferred via exosomes. Therefore, the effects of NETs on VSMCs are spread to VSMCs with no NET contact. Furthermore, we found that TK1 is a key proliferation signaling molecule transferred by exosomes.

Pathological vascular remodeling involves changes in vascular cellular processes, such as vascular cell proliferation, apoptosis, and migration [42–45]. Owing to the high degree of plasticity, dysregulated VSMCs in the medial layer of the vessel wall are the most abundant cell type in the

arterial vessel wall and are the predominant cells contributing to the pathogenesis of systemic hypertension [46,47]. Therefore, targeting dysfunctional VSMCs may have significant implications for the treatment of hypertension. NETs promoted VSMC proliferation, which is related to vascular remodeling and hypertension. Additionally, NET formation was induced with PMA in mouse vessels. An increase in blood pressure increase was accompanied by NETosis in the small arteries of mice. NETs, therefore, was related to hypertension. Alternatively, we also demonstrated that hypertension contributed to NETosis in arteries. This is probably because of a mechanical damage to the vascular wall, which is conducive to the infiltration of neutrophils and NETosis. It is important to note that vascular remodeling related to hypertension is influenced by factors with a complex underlying mechanism. In this study, we only evaluated the effects of NETs on VSMCs. The effects of NETs on other vascular cells and the extracellular matrix should be explored in future studies.

Further, as the blood pressure increased, TK1 expression was increased in the serum of mice with PMA-induced NETosis. In cancer research, TK1 is a marker used to screen tumors, assess the response to therapy, and evaluate prognosis [48,49]. Our results extend the clinical application of TK1 by indicating that it is not only upregulated in tumors but also in benign diseases related to proliferation. The degree of TK1 up-regulation may differ among diseases and the quantification of TK1 changes in different diseases is an important topic for future research. There was no significant difference in the expression of TK1 in the serum of SHR and WKY, and there were significant individual differences in the expression of TK1 both in SHR group and WKY group. We analyze the reason is the small number of animals and differences in individual state of animals. In future experiment, we will expand the number of animals and conduct paired samples to detect the relationship between blood pressure and TK1 expression.

Broadly, our results indicate that the phenotypic alteration of VSMCs induced by NETs is a pathogenic factor in hypertension and is a promising target for antihypertensive therapy. On the basis of these findings, the management of hypertension should be largely focused on limiting the progression of complications by targeting precise pathophysiological mechanisms, such as inflammation and the vascular structure, rather than blood pressure control alone, which fails to markedly reduce the risk for vascular complications and mortality. Though more experiments are needed to explore, NETs probably become a target for prevention and treatment of hypertension.

ACKNOWLEDGEMENTS

Funding: this work was supported by the National Natural Science Foundation of China (grant no. 81900372, 81970254, 81800381, 81970211, 30640003) and Science and Technology Design Program of the Science and Technology Agency of Liaoning Province, China (grant no. 2011225027).

Conflicts of interest

There are no conflicts of interest.

REFERENCES

1. Lacruz ME, Kluttig A, Hartwig S, Löer M, Tiller D, Greiser KH, *et al.* Prevalence and incidence of hypertension in the general adult population results of the CARLA-Cohort Study. *Medicine (Baltimore)* 2015; 94:e952.
2. Qi SF, Zhang B, Wang HJ, Yan J, Mi YJ, Liu DW, *et al.* Prevalence of hypertension subtypes in 2011 and the trends from 1991 to 2011 among Chinese adults. *J Epidemiol Community Health* 2016; 70:444–451.
3. Levy E, Spahis S, Bigras JL, Delvin E, Borys JM. The epigenetic machinery in vascular dysfunction and hypertension. *Curr Hypertens Rep* 2017; 19:52.
4. Bavishi C, Bangalore S, Messerli FH. Outcomes of intensive blood pressure lowering in older hypertensive patients. *J Am Coll Cardiol* 2017; 69:486–493.
5. Luo Q, Zhang Y, Yang X, Qin L, Wang H. Hypertension in connective tissue disease. *J Hum Hypertens* 2022; May 3:.
6. Agita A, Alsagaff MT. Inflammation, immunity, and hypertension. *Acta Med Indones* 2017; 49:158–165.
7. Vinh A, Drummond GR, Sobey CG. Immunity and hypertension: new targets to lighten the pressure. *Br J Pharmacol* 2019; 176:1813–1817.
8. Herrero-Cervera A, Soehnlein O, Kenne E. Neutrophils in chronic inflammatory diseases. *Cell Mol Immunol* 2022; 19:177–191.
9. Rudnicka E, Suchta K, Grymowicz M, Calik-Ksepka A, Smolarczyk K, Duszewska AM, *et al.* Chronic low grade inflammation in pathogenesis of PCOS. *Int J Mol Sci* 2021; 22:3789.
10. Mohammed S, Thadathil N, Selvarani R, Nicklas EH, Wang D, Miller BF, *et al.* Necroptosis contributes to chronic inflammation and fibrosis in aging liver. *Aging Cell* 2021; 20:e13512.
11. Cahilog Z, Zhao H, Wu L, Alam A, Eguchi S, Weng H, *et al.* The role of neutrophil NETosis in organ injury: novel inflammatory cell death mechanisms. *Inflammation* 2020; 43:2021–2032.
12. Lok LSC, Dennison TW, Mahbubani KM, Saeb-Parsy K, Chilvers ER, Clatworthy MR. Phenotypically distinct neutrophils patrol uninfected human and mouse lymph nodes. *Proc Natl Acad Sci U S A* 2019; 116:19083–19089.
13. Wong SL, Demers M, Martinod K, Gallant M, Wang Y, Goldfine AB, *et al.* Diabetes primes neutrophils to undergo NETosis, which impairs wound healing. *Nat Med* 2015; 21:815–819.
14. Kazzaz NM, Sule G, Knight JS. Intercellular interactions as regulators of NETosis. *Front Immunol* 2016; 7:453.
15. Sollberger G, Tilley DO, Zychlinsky A. Neutrophil extracellular traps: the biology of chromatin externalization. *Dev Cell* 2018; 44:542–553.
16. Dąbrowska D, Jabłońska E, Garley M, Sawicka-Powierza J, Nowak K. The phenomenon of neutrophil extracellular traps in vascular diseases. *Arch Immunol Ther Exp (Warsz)* 2018; 66:273–281.
17. Lu Y, Jiang H, Li B, Cao L, Shen Q, Yi W, *et al.* Telomere dysfunction promotes small vessel vasculitis via the LL37-NETs-dependent mechanism. *Ann Transl Med* 2020; 8:357.
18. Kimball AS, Obi AT, Diaz JA, Henke PK. The emerging role of NETs in venous thrombosis and immunothrombosis. *Front Immunol* 2016; 7:236.
19. Kapoor S, Opneja A, Nayak L. The role of neutrophils in thrombosis. *Thromb Res* 2018; 170:87–96.
20. Aldabbous L, Abdul-Salam V, McKinnon T, Duluc L, Pepke-Zaba J, Southwood M, *et al.* Neutrophil extracellular traps promote angiogenesis: evidence from vascular pathology in pulmonary hypertension. *Arterioscler Thromb Vasc Biol* 2016; 36:2078–2087.
21. Suzuki M, Ikari J, Anazawa R, Tanaka N, Katsumata Y, Shimada A, *et al.* PAD4 deficiency improves bleomycin-induced neutrophil extracellular traps and fibrosis in mouse lung. *Am J Respir Cell Mol Biol* 2020; 63:806–818.
22. Harvey A, Montezano AC, Lopes RA, Rios F, Touyz RM. Vascular fibrosis in aging and hypertension: molecular mechanisms and clinical implications. *Can J Cardiol* 2016; 32:659–668.
23. Xia X, Zhang Z, Zhu C, Ni B, Wang S, Yang S, *et al.* Neutrophil extracellular traps promote metastasis in gastric cancer patients with postoperative abdominal infectious complications. *Nat Commun* 2022; 13:1017.
24. Yang M, Chen Q, Mei L, Wen G, An W, Zhou X, *et al.* Neutrophil elastase promotes neointimal hyperplasia by targeting toll-like receptor 4 (TLR4)-NF-κB signalling. *Br J Pharmacol* 2021; 178:4048–4068.

25. Schroder AL, Chami B, Liu Y, Doyle CM, El Kazzi M, Ahlenstiel G, *et al*. Neutrophil extracellular trap density increases with increasing histopathological severity of Crohn's disease. *Inflamm Bowel Dis* 2022; 28:586–598.
26. Wang Y, Li X, Huang X, Ma S, Xing Y, Geng X, *et al*. Sauchinone inhibits angiotensin II-induced proliferation and migration of vascular smooth muscle cells. *Clin Exp Pharmacol Physiol* 2020; 47:220–226.
27. Hoppenbrouwers T, Autar ASA, Sultan AR, Abraham TE, van Cappellen WA, Houtsmuller AB, *et al*. In vitro induction of NETosis: comprehensive live imaging comparison and systematic review. *PLoS One* 2017; 12:e0176472.
28. Lv P, Miao SB, Shu YN, Dong LH, Liu G, Xie XL, *et al*. Phosphorylation of smooth muscle 22**α** facilitates angiotensin II-induced ROS production via activation of the PKC**α**-P47phox axis through release of PKC**α** and actin dynamics and is associated with hypertrophy and hyperplasia of vascular smooth muscle cells in vitro and in vivo. *Circ Res* 2012; 111:697–707.
29. Xie XL, Nie X, Wu J, Zhang F, Zhao LL, Lin YL, *et al*. Smooth muscle 22**α** facilitates angiotensin II-induced signaling and vascular contraction. *J Mol Med (Berl)* 2015; 93:547–558.
30. Kodigepalli KM, Bonifati S, Tirumuru N, Wu L. SAMHD1 modulates in vitro proliferation of acute myeloid leukemia-derived THP-1 cells through the PI3K-Akt-p27 axis. *Cell Cycle* 2018; 17:1124–1137.
31. Simons M, Raposo G. Exosomes–vesicular carriers for intercellular communication. *Curr Opin Cell Biol* 2009; 21:575–581.
32. Meldolesi J. Exosomes and ectosomes in intercellular communication. *Curr Biol* 2018; 28:R435–R444.
33. Kalluri R, LeBleu VS. The biology, function, and biomedical applications of exosomes. *Science* 2020; 367:eaau6977.
34. Zhou MS, Schulman IH, Raij L. Nitric oxide, angiotensin II, and hypertension. *Semin Nephrol* 2004; 24:366–378.
35. Watanabe T, Pakala R, Katagiri T, Benedict CR. Angiotensin II and serotonin potentiate endothelin-1-induced vascular smooth muscle cell proliferation. *J Hypertens* 2001; 19:731–739.
36. Chrysanthopoulou A, Gkaliagkousi E, Lazaridis A, Arelaki S, Pateinakis P, Ntinopoulou M, *et al*. Angiotensin II triggers release of neutrophil extracellular traps, linking thromboinflammation with essential hypertension. *JCI Insight* 2021; 6:e148668.
37. Pegtel DM, Cosmopoulos K, Thorley-Lawson DA, van Eijndhoven MA, Hopmans ES, Lindenberg JL, *et al*. Functional delivery of viral miRNAs via exosomes. *Proc Natl Acad Sci U S A* 2010; 107:6328–6333.
38. Weagel EG, Meng W, Townsend MH, Velazquez EJ, Brog RA, Boyer MW, *et al*. Biomarker analysis and clinical relevance of TK1 on the cell membrane of Burkitt's lymphoma and acute lymphoblastic leukemia. *Onco Targets Ther* 2017; 10:4355–4367.
39. Singh S, Kumar R, Kumar U, Kumari R. Clinical significance and role of TK1, CEA, CA 19-9 and CA 72-4 levels in diagnosis of colorectal cancers. *Asian Pac J Cancer Prev* 2020; 21:3133–3136.
40. Jagarlamudi KK, Hansson LO, Eriksson S. Breast and prostate cancer patients differ significantly in their serum Thymidine kinase 1 (TK1) specific activities compared with those hematological malignancies and blood donors: implications of using serum TK1 as a biomarker. *BMC Cancer* 2015; 15:66.
41. Yoon JH, Ashktorab H, Smoot DT, Nam SW, Hur H, Park WS. Uptake and tumor-suppressive pathways of exosome-associated GKN1 proteinin gastric epithelial cells. *Gastric Cancer* 2020; 23:848–862.
42. Dai Z, Zhu MM, Peng Y, Jin H, Machireddy N, Qian Z, *et al*. Endothelial and smooth muscle cell interaction via FoxM1 signaling mediates vascular remodeling and pulmonary hypertension. *Am J Respir Crit Care Med* 2018; 198:788–802.
43. Wang X, Khalil RA. Matrix metalloproteinases, vascular remodeling, and vascular disease. *Adv Pharmacol* 2018; 81:241–330.
44. Sun HJ, Ren XS, Xiong XQ, Chen YZ, Zhao MX, Wang JJ, *et al*. NLRP3 inflammasome activation contributes to VSMC phenotypic transformation and proliferation in hypertension. *Cell Death Dis* 2017; 8:e3074.
45. Lacolley P, Regnault V, Avolio AP. Smooth muscle cell and arterial aging: basic and clinical aspects. *Cardiovasc Res* 2018; 114:513–528.
46. Gollasch M, Welsh DG, Schubert R. Perivascular adipose tissue and the dynamic regulation of Kv 7 and Kir channels: implications for resistant hypertension. *Microcirculation* 2018; 25:e12434.
47. Dai Z, Zhu MM, Peng Y, Machireddy N, Evans CE, Machado R, *et al*. Therapeutic targeting of vascular remodeling and right heart failure in pulmonary arterial hypertension with a HIF-2alpha inhibitor. *Am J Respir Crit Care Med* 2018; 198:1423–1434.
48. Meirovitz A, Gross M, Leibovici V, Sheva K, Popovzer A, Barak V. Clinical applicability of the proliferation marker thymidine kinase 1 in head and neck cancer patients. *Anticancer Res* 2021; 41:1083–1087.
49. Nisman B, Allweis TM, Carmon E, Kadouri L, Maly B, Maimon O, *et al*. Elevated free triiodothyronine is associated with increased proliferative activity in triple-negative breast cancer. *Anticancer Res* 2021; 41: 949–954.